Electron Transfer and Electrocatalytic Properties of the Immobilized Methionine80Alanine Cytochrome *c* Variant

Stefano Casalini,[†] Gianantonio Battistuzzi,[†] Marco Borsari,[†] Carlo Augusto Bortolotti,[‡] Antonio Ranieri,[†] and Marco Sola*[,†,‡]

Department of Chemistry, University of Modena and Reggio Emilia, Via Campi 183, I-41100 Modena, Italy, and CNR-INFM National Center nanoStructures and bioSystems at Surfaces—S3, Via Campi 213/A, I-41100 Modena, Italy

Received: August 16, 2007; In Final Form: November 5, 2007

The M80A variant of yeast iso-1-cytochrome *c* (cytc), which features a noncoordinating Ala residue in place of the axial heme iron Met ligand, was chemisorbed on a gold electrode coated with 4-mercaptopyridine or carboxyalkanethiol self-assembled monolayers (SAM) and investigated by cyclic voltammetry at varying conditions of temperature, pH, and O_2 concentration. The $E^{\circ\prime}$ value (standard reduction potential for the heme Fe(III)/Fe(II) couple) of M80A cytc on both SAMs is of approximately −200 mV (vs the standard hydrogen electrode, SHE) at pH 7, which is more than 400 mV lower than that of native cytochrome *c* in the same conditions. The thermodynamics of Fe(III) to Fe(II) reduction and the kinetics of heterogeneous electron transfer (ET) are dominated by the presence of a hydroxide ion as the sixth axial heme iron ligand above pH 6. On both SAMs, protonation of the bound hydroxide ion is mainly responsible for the changes in these parameters at low pH, since the distances of ET between the heme and the electrode are found to be independent of pH in the range of 5−11. The invariance of the electrochemical features up to pH 11 indicates that no changes in heme iron coordination occur at high pH, at variance with native cytc. Most notably, immobilized M80A cytc is found to act as an efficient biocatalyst for O_2 reduction from pH 5 to 11.0. This finding makes M80A cytc a suitable candidate as a constituent of a biocatalytic interface for O_2 biosensing and opens the way for the exploitation of engineered cytochrome *c* in the bio-based detection of chemicals of environmental and clinical interest.

Introduction

In these last years, several examples of well-behaved electrochemistry in nondenaturing conditions have been reported for cytochrome *c* (cytc) immobilized on bare or functionalized solid electrodes through covalent linkages, hydrogen bonding, or electrostatic interactions.[1−16] Electrode immobilization of redox proteins allows insight to be gained into the mechanism of electron transfer (ET) between protein partners and is a key step for the assembly of biomolecular electronic devices (e.g., biotransistors and biosensors).[17,18] Native and wt recombinant iso-1-cytochrome *c* from *Saccharomyces cerevisiae* (YCC) is considered to be a suitable candidate for bioelectronic applications since it (i) contains a single surface cysteine residue that can be exploited for specific tethering assuring unique orientation of the protein,[19,20] (ii) possesses a large positive charge which allows electrostatic binding to negatively charged self-assembled monolayers (SAM), (iii) is rather stable in a variety of solution conditions, and most importantly, (iv) features a heme environment that can be engineered to mimic that of heme enzymes with specific affinity for a number of chemicals of environmental (CO, NO, NO_2^-, etc.) and clinical (H_2O_2 and hydroperoxides) interest. By now, yeast iso-1-cytc covalently immobilized on gold was found to catalyze O_2 reduction below pH 3.[8] In these conditions, both axial heme iron ligands dissociate,[21] thereby allowing O_2 binding to the ferrous form.[8] The catalytic current being proportional to O_2 concentration, this low-pH cytc conformer could serve as a constituent of a biocatalytic interface for an O_2 biosensor. The obvious limitation of this system is due to the fact that it works only at very acidic pH. Therefore, any cytc variant featuring one or both open axial coordination positions of the heme iron in a large pH range would be worth investigating in this respect. The M80A variant of yeast iso-1-cytochrome *c*, in which the axial heme iron Met ligand is replaced by a noncoordinating Ala residue (M80A hereafter),[21−25] represents the basic species to start with for the production of biosurfaces able to mediate a dioxygen redox chemistry. Although M80A features an OH^- ion as the "sixth" axial heme ligand above pH 6 (Figure 1),[22,25] the Fe(II) form is known to strongly bind dioxygen with a low autoxidation rate.[25]

Here, we have studied the redox properties of M80A chemisorbed on a solid (gold) electrode coated with a negatively charged mixed SAM made of HOOC-alkanethiols and HO-alkanethiols and a 4-mercaptopyridine SAM. Moreover, its ability to catalyze O_2 reduction in these conditions was investigated from pH 5 to 11. The enthalpy and entropy changes of the reduction reaction obtained from variable-temperature $E^{\circ\prime}$ (standard reduction potential for the heme Fe(III)/Fe(II) couple) measurements were also determined, which are illuminating on the molecular determinants of the reduction potential ($E^{\circ\prime}$) in heme proteins. Moreover, we here measured the rate constants of heterogeneous ET of M80A in different conditions which, within the frame of the Marcus theory, allow

* Corresponding author. Tel.: +39 059 2055037. Fax: +39 059 373543. E-mail: marco.sola@unimore.it.
[†] University of Modena and Reggio Emilia.
[‡] CNR-INFM National Center—S3.

10.1021/jp0765953 CCC: $40.75
Published on Web 01/15/2008

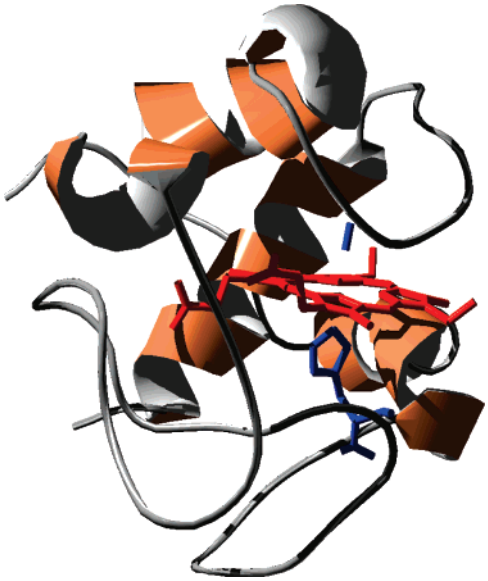

Figure 1. Three-dimensional representation of the averaged MD structure of the M80A/C102T mutant of *S. cerevisiae* iso-1-cytochrome *c*. (Reprinted from ref 22. Copyright 1995 American Chemical Society.) The heme is in red sticks, and the proximal histidine and the OH^- axially bound to Fe(III) are in blue sticks.

insight to be gained on the distance and reorganization energy of ET and therefore on the geometric features of the SAM−protein system. Remarkably, the present results show that immobilized M80A in these conditions is able to catalytically reduce dioxygen over a wide pH range and therefore can in principle be exploited for the amperometric biosensing of O_2.

Experimental Methods

Materials. All chemicals were of reagent grade. 4-Mercaptopyridine (4-MP), 11-mercapto-1-undecanoic acid (11-MUAc), and 11-mercapto-1-undecanol (11-MUAl) (Sigma-Aldrich) were recrystallized from hexane before use. Nanopure water was used throughout.

Protein Production and Isolation. The M80A/C102T mutant of *S. cerevisiae* iso-1-cytochrome *c* was produced using the QuikChange XL site-directed mutagenesis kit (Stratagene) starting from two synthetic oligonucleotide primers carrying the desired mutation and using as DNA template the plasmid pMSV1, which was kindly donated by the late Professor M. S. Viezzoli of the University of Florence. This plasmid expresses the C102T variant of yeast iso-1-cytochrome *c* from the pTrc promotor and confers ampicillin resistance. Therefore, the M80A/C102T variant carries an alanine residue replacing the axial heme iron methionine ligand and a threonine in place of native Cys102. Protein expression in *E. coli* and purification were carried out as described elsewhere.[26]

Electrochemical Measurements. Cyclic voltammetry (CV) experiments were carried out with a potentiostat/galvanostat PAR model 273A at different scan rates (0.02−2 V s^{-1}) using a cell for small-volume samples (0.5 mL) under argon. All experiments were carried out using a 1 mm diameter polycrystalline gold wire as working electrode and a Pt sheet and a saturated calomel electrode (SCE) as counter and reference electrode, respectively. The electric contact between the SCE and the working solution was obtained with a Vycor (PAR) set. Potentials were calibrated against the MV^{2+}/MV^{+} couple (MV = methylviologen).[27] All the redox potentials reported here are referred to the standard hydrogen electrode (SHE). The

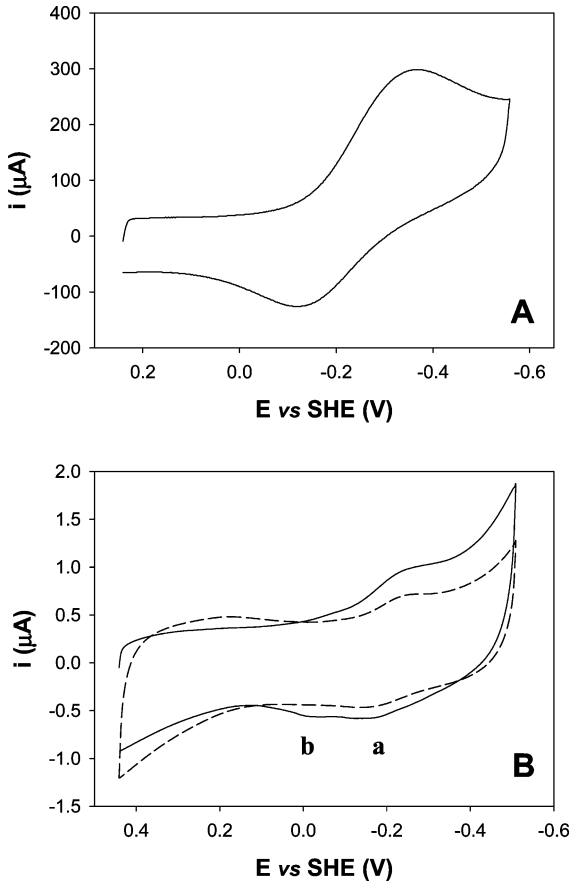

Figure 2. (A) Cyclic voltammogram for M80A/C102T *S. cerevisiae* iso-1-cytochrome *c* immobilized on a polycrystalline gold electrode coated with a 1:1 mixed SAM of 11-MUAc and 11-MUAl in 5 mM phosphate buffer, 5 mM sodium perchlorate, pH 7. Sweep rate, 50 mV s^{-1}. T = 20 °C. (B) Cyclic voltammogram for M80A/C102T *S. cerevisiae* iso-1-cytochrome *c* immobilized on a polycrystalline gold electrode coated with a SAM of 4-mercaptopyridine (4-MP) in 10 mM phosphate buffer, 0.1 M sodium chloride, pH 7. Sweep rate, 50 mV s^{-1}. T = 20 °C. Solid and dashed lines correspond to the 1st and the 20th voltammetric scan, respectively.

working gold electrode was cleaned by flaming it in oxidizing conditions; afterward, it was heated in concentrated KOH for 30 min then, after rinsing in water, in concentrated sulfuric acid for 30 min. To minimize residual adsorbed impurities, the electrode was subjected to 20 voltammetric cycles between +1.5 and −0.25 V at 0.1 V s^{-1} in 1 M H_2SO_4. Finally, the electrode was rinsed in water and anhydrous ethanol. The Vycor set was treated in an ultrasonic pool for about 5 min. The gold electrode was coated with the SAMs of 4-MP and 11-MUAc/11-MUAl by dipping the cleaned electrode into a 1 mM solution of 4-MP in water for 120 s and into a 1 mM ethanolic 1:1 solution of 11-MUAc and 11-MUAl for 12 h at 5 °C, respectively, and then rinsing it with Milli-Q water. A total of 10 CV cycles from +200 mV to −300 mV were then run with the SAM-coated electrodes in a 5 mM sodium perchlorate solution outgassed with argon to set the background and check for the absence of spurious signals.

Protein solutions were freshly prepared before use in 5 mM phosphate buffer at pH 7, and their concentration (typically 50 μM) was checked spectrophotometrically. Protein adsorption on the Au electrode coated with 4-MP and with the mixed carboxyalkanethiolate layer was achieved by dipping the functionalized electrode into the above protein solution for 4 and 24 h, respectively, at 4 °C. All electrochemical experiments on

TABLE 1: Thermodynamic Parameters for Fe(III) to Fe(II) Reduction for M80A/C102T *S. cerevisiae* Iso-1-cytochrome *c* Adsorbed on a Polycrystalline Gold Electrode Coated with a 1:1 Mixed SAM of 11-MUAc and 11-MUAl (MUA) and a SAM of 4-MP at Different pH Values[a]

protein	SAM	pH	$E^{\circ\prime}_{298K}$ (V)	$\Delta H^{\circ\prime}_{rc}$ (kJ mol^{-1})	$\Delta S^{\circ\prime}_{rc}$ (J K^{-1} mol^{-1})	$-\Delta H^{\circ\prime}_{rc}/F$ (V)	$T\Delta S^{\circ\prime}_{rc}/F$ (V)
M80A	4-MP	5.1	−0.092	0	−28	−0.003	−0.087
M80A	4-MP	7.0	−0.194	+13	−21	−0.132	−0.064
M80A	4-MP	11.2	−0.209	+15	−16	−0.161	−0.049
M80A	MUA	5.1	−0.140	+27	+46	−0.281	+0.143
				+2	−39	−0.021	−0.120
M80A	MUA	7.0	−0.201	+42	+78	−0.435	+0.241
wt (C102T)	MUA	7.0	+0.210	−46	−86	+0.477	−0.266

[a] The upper and lower row for M80A cytc on MUA at pH 5 refer to values determined below and above 25 °C, respectively. Values for wt cytc are taken from ref 32.

TABLE 2: Kinetic Constants Measured at Different Temperatures and Calculated Activation Enthalpies for the Heterogeneous Electron Transfer between the Protein and the Electrode for M80A/C102T *S. cerevisiae* Iso-1-cytochrome *c* Immobilized on a Polycrystalline Gold Electrode Coated with a 1:1 Mixed SAM of 11-MUAc and 11-MUAl (MUA) and a SAM of 4-MP at Different pH Values[a]

protein	SAM	k_s (5 °C) (s^{-1})	k_s (20 °C) (s^{-1})	k_s (35 °C) (s^{-1})	$\Delta H^{\ddagger}$ (kJ mol^{-1})	λ (eV)
M80A	4-MP, pH 5.1	6.1	7.1	8.4	7.6	0.315
M80A	4-MP, pH 7.0	1.8	2.2	2.8	10.5	0.435
M80A	4-MP, pH 11.0	1.7	2.2	2.7	11.0	0.456
M80A	MUA, pH 5.1	5.0	6.1	3.1	9.0 (T < 25 °C)	0.373 (T < 25 °C)
M80A	MUA, pH 7.0	1.4	1.9	2.2	10.8	0.448
wt (C102T)	MUA, pH 7.0	39	46	55	8.5	0.353

[a] Values for wt (C102T) cytc are taken from ref 32.

the protein-coated electrodes were performed in 10 or 5 mM phosphate buffer (with 4-MP and mixed 11-MUAc/11-MUAl SAMs, respectively), containing 100 mM sodium chloride (4-MP SAM) or 5 mM sodium perchlorate (mixed carboxyalkanethiolate SAM), as the base electrolyte. The pH was adjusted with slight additions of concentrated HCl or NaOH under fast stirring. For both SAMs, the transfer coefficient α is found to be approximately 0.5 and the equilibrium reduction potentials ($E^{\circ\prime}$) for cytc, calculated from the average of the anodic and cathodic peak potentials, are almost independent of the scan rate in the range of 0.01−2 V s^{-1}. Experiments were repeated at least two times, and the reduction potentials were found to be reproducible within ±2 mV. To estimate the percent surface coverage, the area of the immersed portion of the gold wire was carefully calculated after each CV session by dipping the bare electrode at exactly the same depth into a solution of an electrochemical standard, ferricinium tetrafluoborate, recording the CV signal for the standard, and then applying the Randles−Sevcik relationship. Cyclic voltammograms at variable scan rate were recorded to determine the electron-transfer rate constant k_s for the adsorbed protein, according to the Laviron method.[28] The k_s values were averaged over five measurements and found to be reproducible within ±2 s^{-1}.

Variable-temperature CV experiments were carried out with a cell in a "nonisothermal" setting,[29,30] namely, in which the reference electrode was kept at constant temperature (21 ± 0.1 °C), whereas the half-cell containing the working electrode and the Vycor junction to the reference electrode were kept under thermostatic control with a water bath. The temperature was varied from 5 to 35 °C. With this experimental configuration, the reaction entropy for reduction of the oxidized protein ($\Delta S^{\circ\prime}_{rc}$, entropy change for heme Fe(III) to Fe(II) reduction) is given by[29−31]

$$\Delta S^{\circ\prime}_{rc} = S^{\circ\prime}_{red} - S^{\circ\prime}_{ox} = nF(dE^{\circ\prime}/dT) \quad (1)$$

thus, $\Delta S^{\circ\prime}_{rc}$ was determined from the slope of the plot of $E^{\circ\prime}$ versus temperature which turns out to be linear under the assumption that $\Delta S^{\circ\prime}_{rc}$ is constant over the limited temperature range investigated. With the same assumption, the enthalpy change ($\Delta H^{\circ\prime}_{rc}$, enthalpy change for heme Fe(III) to Fe(II) reduction) was obtained from the Gibbs−Helmholtz equation, namely, as the negative slope of the $E^{\circ\prime}/T$ versus $1/T$ plot. The nonisothermal behavior of the cell was carefully checked by determining the $\Delta H^{\circ\prime}_{rc}$ and $\Delta S^{\circ\prime}_{rc}$ values of the ferricyanide/ferrocyanide couple.[30,31] Average errors on $\Delta H^{\circ\prime}_{rc}$ and $\Delta S^{\circ\prime}_{rc}$ values are ±1 kJ mol^{-1} and ±2 J mol^{-1} K^{-1}, respectively. The electrocatalytic reduction of O_2 by immobilized M80A cytc at different pH values was studied by gradually adding air to the O_2-free solution at normal atmospheric pressure at 20 °C.

Results

A typical cyclic voltammogram for M80A immobilized on a polycrystalline gold electrode coated with a 1:1 mixed SAM of 11-MUAc and 11-MUAl (MUA hereafter) is shown in Figure 2A. No CV response has been observed for the SAM-coated electrodes in the absence of protein. For immobilized M80A, a single feature is observed, which originates from the one-electron reduction/oxidation of the M80A heme iron. The peak current ratio $i_{anodic}/i_{cathodic}$ is approximately 1 for all the temperatures and scan rates investigated (see below). Peak currents linearly increase with increasing scan rate (not shown) indicating that the electrochemical response originates from M80A immobilized onto the electrode. The $E^{\circ\prime}$ value of −201 mV at pH 7 and 25 °C is about 400 mV more negative than that observed for the wild-type (His, Met-ligated) form of the protein adsorbed on the same SAM (Table 1).[32−36] The electrochemical response is remarkably stable at neutral and moderately acidic pH values (down to pH 5) and persists after many voltammetric cycles (at least 20) throughout the temperatures range investigated. Peak separation increases with

increasing scan rate and temperature. The signal intensity decreases upon increasing the ionic strength and the pH of the solution. In particular, at pH 7, the signal disappears for NaCl concentrations higher than 0.5 M and no electrochemical response could be obtained at pH values above 9. The former effect indicates that the protein−SAM interaction is mainly electrostatic, whereas the latter is probably a consequence of the weakening of such an interaction due to surface Lys deprotonation.

The electrochemistry of M80A on the 4-MP SAM is distinctive (Figure 2B). The first-scan voltammogram (Figure 2B, solid line) contains two signals (*a* and *b*). The weaker signal *b*, falling at more positive potentials, disappears after some reduction/oxidation cycles (Figure 2B, dashed line). Since M80A is the only electroactive species within the range of potentials analyzed, it appears that the protein exists in two forms with different reduction potentials, one of which either becomes electroinactive or disappears after repeated reduction/oxidation cycles. In general, this behavior is observed when the freely diffusing and the surface-adsorbed forms of the protein coexist. In fact, repeated cathodic/anodic scans increase the surface coverage of the protein, which acts as an obstacle to the heterogeneous electron transfer with the freely diffusing species.[37] Indeed, the peak current of signal *a* linearly increases with increasing the scan rate (υ) (not shown) indicating that the electrochemical response originates from immobilized M80A, whereas the current of signal *b* linearly increases with $\upsilon^{1/2}$, typical of a diffusive process. Due to its nature, signal *b* will not be considered further. The cathodic and anodic peaks of the adsorbed protein are separated by approximately 100 mV at a scan rate of 50 mV s^{-1} (Figure 2B). Peak separation increases with increasing scan rate and temperature. The peak current ratio $i_{anodic}/i_{cathodic}$ is approximately 1 for all the temperatures and scan rates investigated. This signal is quite robust; in fact it persists at all the temperatures analyzed after many voltammetric cycles and also after repeatedly dipping the protein-coated electrode in the buffer solution. Moreover, currents are almost unaffected by ionic strength (up to 1 M in NaCl). The $E^{\circ\prime}$ value of −194 mV at pH 7 and 25 °C is closely similar to that observed with MUA (Table 1).

The temperature dependence of the $E^{\circ\prime}$ value for M80A immobilized on MUA at pH 5.1 and 7.0 and on the 4-MP SAM at pH 5.1, 7.0, and 11.0 is shown in Figure 3. The $E^{\circ\prime}/T$ profiles are strongly influenced by the nature of the SAM. A monotonic linear decrease in $E^{\circ\prime}$ with increasing temperature is observed for the 4-MP SAM, independently of pH. For the mixed carboxyalkanethiol SAM at pH 7.0 the $E^{\circ\prime}$ linearly increases with increasing temperature, whereas at pH 5.1 a biphasic $E^{\circ\prime}/T$ profile is observed. The $E^{\circ\prime}$ values and the reduction thermodynamics for M80A adsorbed on the two SAMs at different pH values are listed in Table 1. Reduction of M80A is invariably accompanied by positive $\Delta H^{\circ\prime}_{rc}$ values, which tend to increase with increasing pH, whereas the magnitude and sign of the reduction entropy is SAM-dependent (Table 1). The $E^{\circ\prime}$ of M80A experiences a significant increase upon lowering the pH from 7.0 to 5.1, whose extent is SAM-dependent ($\Delta E^{\circ\prime}$ values of +61 and +102 mV are observed for the carboxyl-terminated and the 4-MP SAM, respectively), whereas the pH increase from 7.0 to 11.2 has a little effect on the $E^{\circ\prime}$ of M80A immobilized on the 4-MP SAM ($\Delta E^{\circ\prime} = -15$ mV).

The surface coverages for M80A chemisorbed on 4-MP and MUA amount to 17.5 and 16.8 ± 0.8 pmol/cm^2, respectively. These values, determined from the overall charge exchanged (evaluated from the area of the baseline-corrected anodic or cathodic peak), correspond to approximately 90% of a full densely packed monolayer (19 pmol/cm^2, as estimated from the crystallographic dimensions of the protein).[7,38]

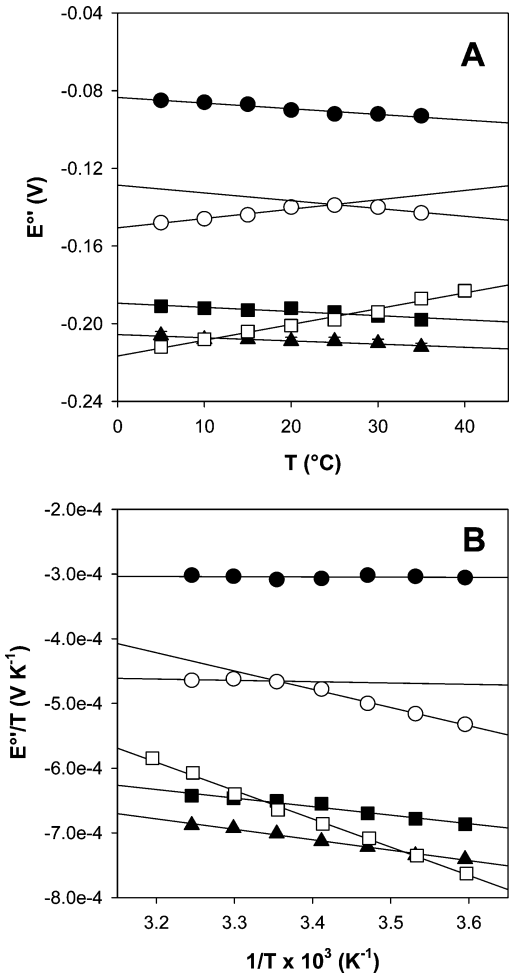

Figure 3. $E^{\circ\prime}$ vs T (A) and $E^{\circ\prime}/T$ vs $1/T$ (B) plots for M80A/C102T *S. cerevisiae* iso-1-cytochrome *c* adsorbed on a polycrystalline gold electrode coated with a 1:1 mixed SAM of 11-MUAc and 11-MUAl (open symbols) and a SAM of 4-MP (filled symbols) at different pH values: pH 5 (●), pH 7 (■), pH 11.2 (▲). Solid lines are least-squares fits to the data points.

The rate constant for the electron transfer between the heme of the adsorbed M80A and the electrode, k_s, are listed in Table 2 along with the activation enthalpies ($\Delta H^{\ddagger}$) calculated from the Arrhenius equation:

$$k_s = A' \exp(-\Delta H^{\ddagger}/RT) \qquad (2)$$

namely, from the slope of the log k_s versus $1/T$ (Figure 4). The error on $\Delta H^{\ddagger}$ is ±0.6 kJ mol^{-1}.

The effect of dioxygen on the electrochemistry of immobilized M80A at pH 5.1 and 7.0 (measurements could be extended to pH 10.0 only for the 4-MP SAM) was studied by recording the CV response at increasing O_2 concentration in the electrochemical cell, as previously reported for cytochrome P450 and the acidic form of native cytochrome *c* covalently attached to a gold electrode.[8,39] Electrocatalytic O_2-reduction waves are observed (Figures 5 and 6), which indicate that the layer formed by the M80A mutant adsorbed on both SAMs acts as a biocatalytic interface for dioxygen reduction at all pH values investigated. In both cases, CV experiments carried out after dioxygen removal were featureless. This is possibly a conse-

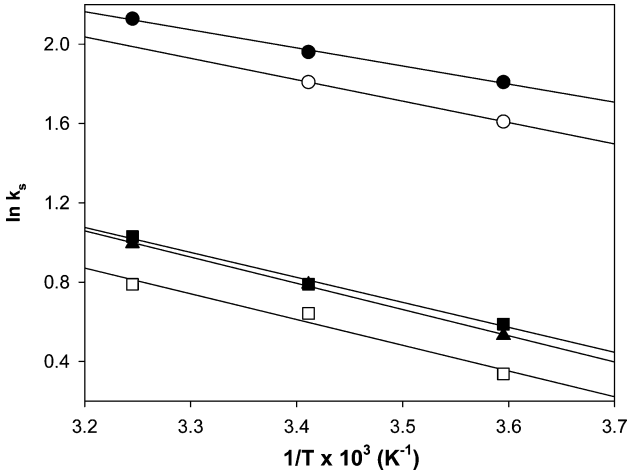

Figure 4. Arrhenius plots for M80A/C102T *S. cerevisiae* iso-1-cytochrome *c* expressed in *E. coli* immobilized on a polycrystalline gold electrode coated with a SAM of 4-mercaptopyridine (4-MP) in 5 mM phosphate buffer, 5 mM sodium perchlorate (filled symbols) or with a 1:1 mixed SAM of 11-MUAc and 11-MUAl in 5 mM phosphate buffer, 5 mM sodium perchlorate (open symbols), pH 7.0 (■, □), pH 5.1 (●, ○), pH 11.2 (▲). Solid lines are least-squares fits to the data points.

quence of oxidative SAM disruption caused by the superoxide ion formed upon dioxygen reduction, which causes protein desorption.

Discussion

Electrochemical Response of M80A. Gold electrodes coated with SAMs made of carboxyalkanethiols and 4-MP are largely used to investigate the redox properties of surface-immobilized and freely diffusing cytochrome *c*, respectively.[32−36,40] In the former case, the negatively charged carboxylate groups of the SAM bind electrostatically to the positively charged surface lysines. In the latter, 4-MP weakly interacts with the protein molecules through H-bond networks involving the pyridine nitrogen and, possibly, solvent molecules. The effects of pH and ionic strength on the electrochemical response of M80A reported here are consistent with these interaction schemes. However, it appears that M80A features a much larger affinity for the 4-MP monolayer compared to the native protein. The molecular determinants of this effect are not at hand. The structural data indicate that residue substitution creates a cavity in the distal zone of the heme, with very limited effects on the residues nearby (Figure 1) and on the overall three-dimensional structure of the protein.[22] However, it is conceivable that removal of the covalent bond between the heme Fe and the S atom of the axial methionine enhances the conformational mobility and the solvent accessibility of the portion of the protein surrounding the mutated residue, thereby strengthening the H-bonding network connecting the solvated protein with the 4-MP monolayer. The heme−electrode distance estimated from the kinetic data (see below) is consistent with this picture.

The $E^{\circ\prime}$ values for immobilized M80A on both SAMs at pH 7 are about 400−500 mV lower than that for the native protein either freely diffusing or covalently/electrostatically immobilized on bare or HOOC-terminated SAM-coated gold electrodes.[32−36,40] The $E^{\circ\prime}$ decrease is to be ascribed for the most part to the stabilization of the ferriheme due to the "hard" hydroxide ion serving as the "sixth" axial heme ligand in M80A at pH 7 in place of the "soft" methionine thioether sulfur in native cytc. The slightly lower $E^{\circ\prime}$ value for M80A at pH 7 on the negatively charged carboxyl-terminated SAM with respect to the 4-MP

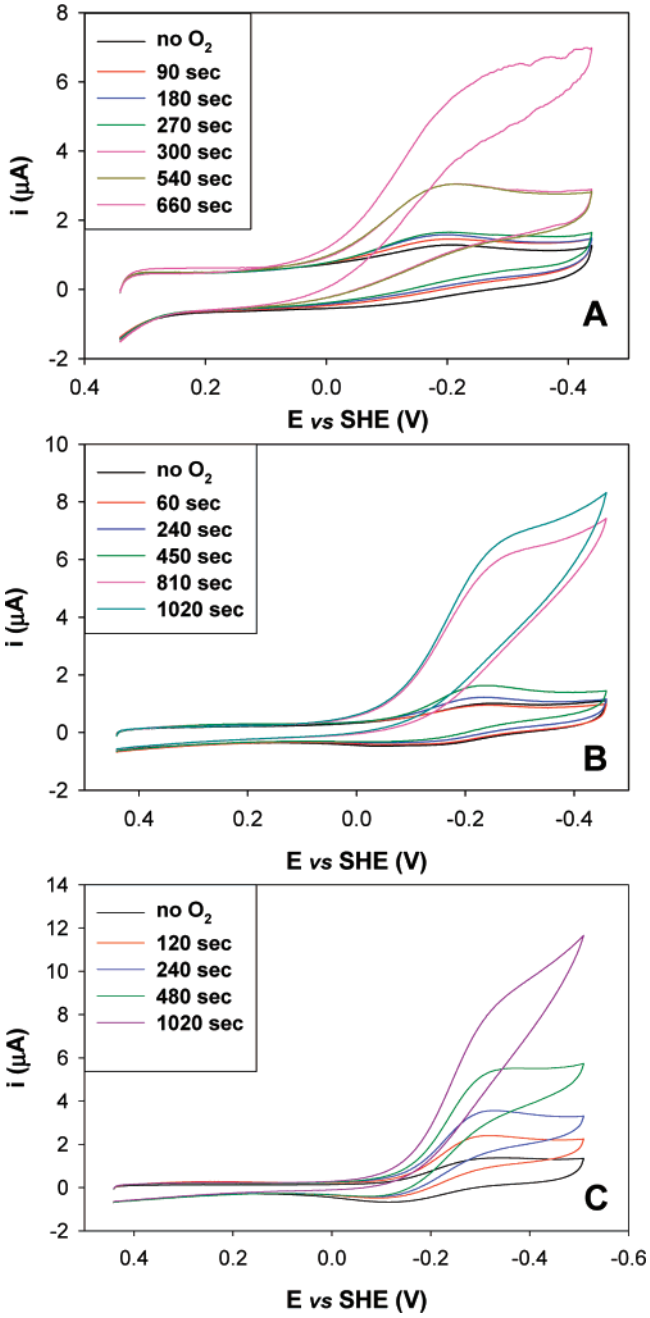

Figure 5. Cyclic voltammograms at different pH values for the M80A/C102T mutant of *S. cerevisiae* iso-1-cytochrome *c* immobilized on a polycrystalline gold electrode coated with a SAM of 4-MP at pH 5 (A), 7 (B), and 10 (C), recorded at different exposure times of the electrochemical cell (initially under argon) to air at normal atmospheric pressure. Sweep rate, 20 mV s^{-1}. $T = 20$ °C.

monolayer (−201 mV vs −194 mV) can be attributed to the electrostatic stabilization of the oxidized form of the M80A mutant, as previously noted for native cytc.[32]

Reduction Thermodynamics. In heme proteins, the reduction enthalpy is mainly controlled by axial heme ligation and the electrostatic interactions between the heme and the protein environment and the solvent.[41−47] The reduction entropy is contributed mostly by reduction-induced solvent reorganization effects and oxidation state-dependent differences in protein flexibility.[41−47] In particular, the negative reduction enthalpy of native cytochrome *c*, either freely diffusing or surface-immobilized, originates from the soft base properties of the thioether sulfur of the axial methionine and from the rather

hydrophobic environment surrounding the heme and its low solvent accessibility which selectively stabilizes the uncharged ferroheme over the positively charged ferric form.[41−47] Since the reduction-induced changes in conformational degrees of freedom of the polypeptide chain in cytochrome *c* are small,[48,49] the reduction entropy is contributed almost entirely by solvent reorganization effects, namely, the reduction-induced changes in the H-bonding network within the hydration sphere of the protein.

Spectroscopic data show that reduction of ferric M80A causes the release of the axial ligand which had replaced the native methionine:[23,24,50,51]

$$\text{M80AFe(III)} - \text{L} + e^- \rightarrow \text{M80AFe(II)} + \text{L} \qquad (3)$$

The ability of immobilized M80A to mediate the electrocatalytic reduction of dioxygen (see below) suggests that the above reaction takes place also upon protein adsorption onto the electrode. In the absence of strong hexogenous heme iron ligands, the axial ligand L is a hydroxide ion which protonates with a pK_a of 5.6.[21,23,24] Therefore, the reduction reactions of immobilized M80A in the present experimental conditions are

$$\text{M80AFe(III)} - OH^- + e^- \rightarrow \text{M80AFe(II)} + OH^-$$

at pH 7 and 11

$$\text{M80AFe(III)} - H_2O + e^- \rightarrow \text{M80AFe(II)} + H_2O$$

at pH 5.1

1:1 Mixed SAM of 11-MUAc and 11-MUAl. At pH 7, replacement of the axial methionine with a noncoordinating alanine has opposing thermodynamic effects. Heme iron reduction is heavily disfavored on enthalpic grounds, but is entropically favored, although to a much lesser extent. The relevant enthalpic stabilization of the oxidized form of the M80A mutant compared to native cytc at pH 7 [$\Delta\Delta H^{\circ\prime}_{rc} = +88$ kJ mol^{-1}, corresponding to an $E^{\circ\prime}$ decrease by 912 mV] is mostly the result of the S(Met)/OH$^-$ ligand substitution leading to the selective stabilization of the Fe(III), as mentioned above. The increased solvent accessibility of the heme distal site in the M80A mutant, which electrostatically stabilizes the positively charged ferric heme, and the reduction-induced dissociation of the axial OH$^-$ ligand further contribute to the positive $\Delta H^{\circ\prime}_{rc}$ value.

Given the negligible effects that replacement of the axial methionine by a noncoordinating alanine residue has on the three-dimensional structure of cytochrome *c*,[22] it is conceivable that the changes in conformational degrees of freedom of the protein matrix due to electron uptake are small as in the native protein. Hence, reduction entropy in M80A appears to be contributed mostly by solvent reorganization effects within the hydration sphere of the protein. The increase of the reduction entropy for M80A with respect to wt cytc is in agreement with the reduction−induced dissociation of the axial hydroxide ligand and with the increased solvent accessibility of the heme as compared to wt cytc.[42−47]

The biphasic $E^{\circ\prime}/T$ profile at pH 5.1 indicates that M80A exhibits different reduction thermodynamics below and above 25 °C. This behavior cannot be interpreted unambiguously due to the absence of spectroscopic data for immobilized M80A cytc. However, by analogy with the same effect observed for several cytochromes *c* in freely diffusing conditions,[47] this effect could be ascribed to a *T*-induced conformational change, possibly triggered by a residue ionization (with a strongly *T*-dependent pK_a).

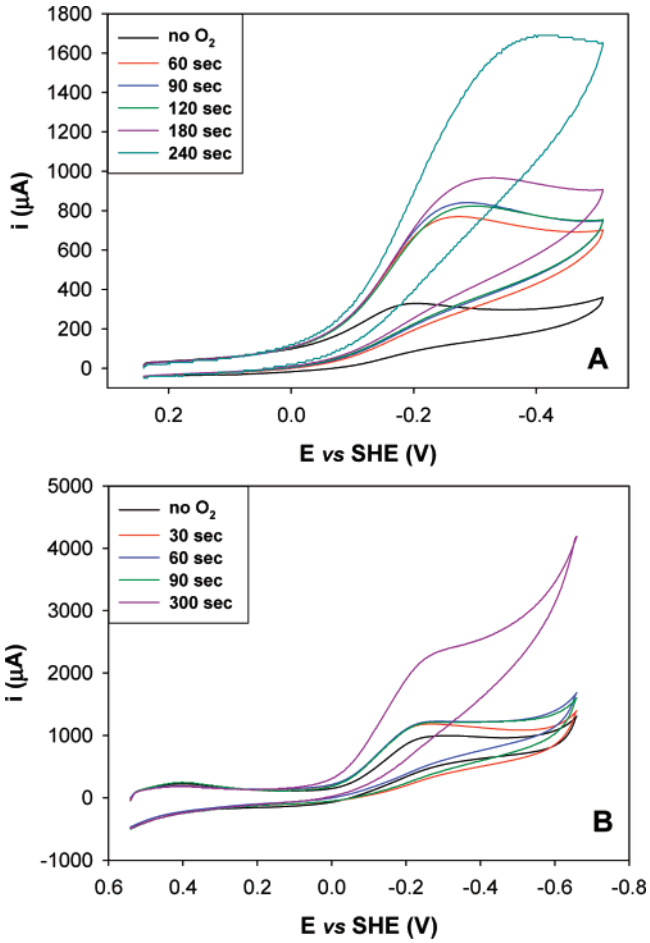

Figure 6. Cyclic voltammograms at different pH values for the M80A/C102T mutant of *S. cerevisiae* iso-1-cytochrome *c* immobilized on a polycrystalline gold electrode coated with a SAM of 1:1 11-MUAc and 11-MUAl at pH 5.2 (A) and 7 (B), recorded at different exposure times of the electrochemical cell (initially under argon) to air at normal atmospheric pressure. Sweep rate, 20 mV s^{-1}. $T = 20$ °C.

The $E^{\circ\prime}$ increase by 61 mV observed upon lowering the pH from 7.0 to 5.1 has an enthalpic origin (the $\Delta H^{\circ\prime}_{rc}$ values become less positive) (Table 1) and can be rather confidently ascribed to the protonation of the OH$^-$ ion axially bound to the Fe(III). The axial water molecule is known indeed to feature a pK_a value of approximately 6,[21,23,24] which apparently is not affected by protein immobilization. Therefore, at pH 5.1 the axial coordination position of the heme Fe(III) is occupied by a water molecule, which is much less efficient in stabilizing the ferric heme than the hydroxide ion.

4-Mercaptopyridine SAM. The reduction thermodynamics sensibly differ from those measured on the 11-MUAc/11-MUAl mixed SAM (Table 1). At both pH 7 and 5.1 the reduction enthalpy is less positive on 4-MP SAM: the decreased enthalpic stabilization of the ferric form in these conditions is consistent with the absence of the electrostatic interactions between the positively charged protein and the carboxylate groups of the SAM. The difference between the $\Delta S^{\circ\prime}_{rc}$ values suggests that the different nature of the interaction between the protein and the two layers deeply influences the reduction-induced solvent reorganization effects within the hydration sphere of M80A cytc.

A pH lowering from 7.0 to 5.1 induces a remarkable increase in $E^{\circ\prime}$ for M80A, as observed for the mixed carboxyalkanethiolate SAM. The close similarity of the enthalpic component of such a $\Delta E^{\circ\prime}$ measured on the two different SAMs suggests that the molecular determinant is the same, namely, the protonation

of the OH^- axially bound to the Fe(III). On the other hand, a pH increase from 7 to 11.2 induces a small decrease in $E^{\circ\prime}$, possibly due to the electrostatic effects of the deprotonation of surface lysines. NMR data suggest that M80A in solution experiences substitution of the bound hydroxide ion by a surface lysine with an apparent pK_a of 10.0, which is made possible by a large conformational rearrangement.[21] For chemisorbed M80A, the almost invariance of both reduction enthalpy and entropy (hence of $E^{\circ\prime}$) from pH 7 to 11 is scarcely compatible with the occurrence of such a large conformational change, although the presence of compensatory molecular effects cannot be excluded. Therefore, although a conclusive evidence is not provided, the M80A mutant immobilized on 4-MP SAM appears not to undergo the alkaline transition, at variance with the protein in solution. This difference could be the result of the decrease in the conformational freedom of the M80A molecules caused by the lateral confinement imposed by the immobilization within the protein monolayer.

Kinetics of the Electron-Transfer Reaction. As shown by Bowden and co-workers, the k_s values obtained with the Laviron method can be assumed to correspond to the kinetic constant for ET at zero driving force.[4,34,52] Therefore, the Marcus equation for heterogeneous ET[53]

$$k_{ET} = \nu_0 \exp[-\beta(r - r_0)] \exp[\pm(F\eta + \lambda)^2/(4\lambda RT)] \quad (4)$$

(where η is the applied overpotential, the other parameters have the usual meaning, and the signs + and − refer to the reduction and oxidation reaction, respectively), in conditions of $\Delta G^{\circ\prime} = F\eta = 0$, assumes the form

$$k_s = \nu_0 \exp[-\beta(r - r_0)] \exp[-\lambda/(4RT)] \quad (5)$$

Since

$$k_s = \nu_0 \exp[-\beta(r - r_0)] \exp[-(\Delta G^{\ddagger}/(RT))] \quad (6)$$

we obtain

$$\Delta G^{\ddagger} = \lambda/4 \quad (7)$$

Since the activation entropy in these systems is in general negligible,[34,54] $\Delta G^{\ddagger}$ can be assumed to correspond to $\Delta H^{\ddagger}$. Therefore, the reorganization energy λ for the immobilized protein can be calculated. The estimated error affecting the λ values is ±0.03 eV. The k_s, $\Delta H^{\ddagger}$, and λ values determined for M80A immobilized on the two SAMs at pH 7 are closely similar (Table 2). The rate constants are lower than those obtained for native yeast and horse heart cytochromes *c* adsorbed on carboxyl-terminated SAMs in similar conditions.[6,33,36,40,57−60] M80A also features larger activation enthalpies and reorganization energies than wt cytc.[34] For the two SAMs, the k_s values increase to a similar extent upon lowering the pH from 7.0 to 5.1, and a parallel decrease in $\Delta H^{\ddagger}$ and λ is observed (Table 2). Almost no changes in the kinetics of ET occur from pH 7.0 to 11.0 on the 4-MP SAM.

These data show that, although the nature of the SAM influences the reduction thermodynamics, it affects only slightly the kinetics of ET. Thus, apparently the decreased electron-transfer efficiency of the M80A mutant compared to the native protein is mainly related to protein-based effects. In particular, it is conceivable that at pH 7.0 the reduction-induced dissociation of the axial hydroxide ligand (eq 1) increases both $\Delta H^{\ddagger}$ and λ compared to wt cytc in similar conditions. Accordingly, the ET efficiency of M80A increases at pH 5, in conditions in which a water molecule serves as axial ligand, whose binding strength is much less affected by the redox state of the heme iron. Moreover, protein features may also affect the distance of ET, as described below. We note that the invariance of the ET kinetics measured on 4-MP SAM from pH 7 to 11 supports the hypothesis offered from the above thermodynamic data that heme axial ligation of immobilized M80A is conserved in this pH range.

Distance of Electron Transfer. The distance of ET between the heme and the electrode (r) for M80A immobilized on MUA at pH 7.0 and 5.1 can be evaluated from the linearized form of eq 6:[4,34]

$$\ln k_s = \ln \nu_0 + [-\beta(r - r_0)] - \Delta G^{\ddagger}/(RT) \quad (8)$$

using a β value of 1 $Å^{-1}$, which is applicable to electron tunneling through the chain of alkane-thiolate-carboxylic acids and the protein matrix,[34,55,56] and an r_0 value of 3 Å.[4,34,53] An r value of 26.9 ± 0.4 Å is obtained for both pH values (the uncertainty on r has been calculated from the absolute errors affecting $\ln k_s$ and $\Delta G^{\ddagger}/RT$). Hence, assigning the chain of 11-MUAc and 11-MUAl a tunneling distance of 19 Å,[6,36] the solvent-exposed heme edge and the SAM surface would come up to 7.9 ± 0.4 Å. This distance is fully consistent with that obtained for wt cytc and its Lys to Ala variants in the same conditions (6.5 and 7.9 ± 0.4 Å, respectively).[32] Although distance differences must be taken cautiously, being significant only within the limits of applicability of the model, the apparently larger tunneling distances for the mutated species would be consistent with the decreased positive protein charge (either due to Lys removal or to hydroxide binding to the ferric heme in M80A) which would result in a weakened electrostatic interaction with the negatively charged SAM.[32]

In the case of the 4-MP SAM, the medium separating the heme and the electrode surface cannot be considered homogeneous, being formed by portions with different β values. This effect can be accounted for by partitioning the first exponential term of eq 8 into a number of components, namely,[2]

$$k_s = \nu_0 \exp[-\textstyle\sum_i(\beta_i r_i) + r_0] \exp[-\Delta H^{\ddagger}/(RT)] \quad (9)$$

where β_i and r_i correspond to the tunneling factor and the thickness of the ith medium component (region), respectively, and the tunneling factor relative to r_0 is considered to be 1 $Å^{-1}$.[4,34,53] For the M80A cytc immobilized on the 4-MP SAM, at least four different regions must be considered. The first two regions correspond to the sulfur atom of 4-MP, covalently linked to the electrode surface, and to the aromatic pyridine moiety. The third region corresponds to the interface between the protein and the 4-MP layer, which contains the H-bonds responsible of the adsorption of the (solvated) protein on the SAM. The protein matrix between the heme edge and the protein surface constitutes the fourth region. In general, for the above regions, the following β_i and r_i are used: $\beta_1 = 1.1$ $Å^{-1}$, $r_1 = 2$ Å;[2,61] $\beta_2 = 0.4$ $Å^{-1}$, $r_2 = 5$ Å;[2,62] $\beta_3 = 2$ $Å^{-1}$, r_3 can vary from 1 to several angstroms, depending on the number of solvation water molecules involved;[2,61] $\beta_4 = 1.4$ $Å^{-1}$, $r_4 = 5$ Å, considering the most favorable orientation.[2,4,61,63]

The linearized form of eq 8 can be used to evaluate r_3:

$$\ln k_s = \ln \nu_0 - (\beta_1 r_1 + \beta_2 r_2 + \beta_3 r_3 + \beta_4 r_4) + r_0 - \Delta H^{\ddagger}/(RT) \quad (10)$$

Assuming $\nu_0 = 10^{12}$ s^{-1} (as suggested for rigid spacers covalently linked to an electrode surface, as 4-MP)[63,64] and r_0

= 3 Å,[4,34,53] the thickness of the interface between the protein and the 4-MP SAM results to be 6.5, 6.1, and 6.1 Å at pH 5.1, 7.0, and 11.0, respectively. These values, almost independent of pH, are consistent with the presence of at least one water molecule at the interface between the M80A cytc and the 4-MP layer.

The fact that the distance of closest approach, *r*, of M80A to the negatively charged MUA and the thickness of the interface between the protein and the 4-MP layer, r_3, are independent of pH indicate that the pH-induced changes in the ET rate cannot be ascribed to alterations in the protein−SAM interaction but mostly to the above-mentioned differences in the coordination sphere of the heme Fe(III).

Interaction of Immobilized M80A with Dioxygen. Replacement of heme redox enzymes by modified ET proteins for biosensing is an extremely promising field of investigation.[66,67] In particular, the advantages of a modified cytc as a constituent of a biosensor for O_2 as compared to a larger heme enzyme include (i) a better electrical communication between the redox center and the electrode, due to the presence of internal electronic pathways evolutionary poised to allow fast electron exchange between redox partners, (ii) the covalent binding of the heme to the protein matrix that prevents heme detachment in an hostile environment (e.g., in the presence of organic solvents), (iii) the stability over a wide range of *T* and pH, and (iv) the availability of a functionally tunable system (through SDM) for increasing activity and optimize performances.

The electrocatalytic O_2-reduction waves observed in the cyclic voltammograms for M80A recorded at different O_2 pressures on both SAMs (Figures 5 and 6) indicate that immobilized M80A can induce the catalytic reduction of dioxygen at all the pH values analyzed. Hence, replacement of the axial methionine with a noncoordinating alanine residue considerably extends the pH range in which cytc acts as an efficient biocatalyst for O_2 reduction, which for the native protein is limited to pH values lower than 3.[8] This is most likely related to the high affinity of dioxygen for the ferrous heme and the concomitant reduction-induced weakening of the axial bond of the water molecule or the hydroxide ion (below and above pH 6, respectively) to the heme iron which favors ligand substitution. The mechanism for O_2 reduction likely implies an oxidative addition of O_2 to Fe(II), as in the case of myoglobin, yielding a Fe(III)$-O_2^-$ derivative, which then dissociates. The loss of the biocatalytic effect of the protein layer after prolonged electrochemistry in the presence of dioxygen could be put in relation with oxidation of both SAMs caused by the superoxide anion (which would result in protein desorption), although there is no clear evidence for it and other factors could be involved. It is a fact that the catalytic surface cannot be renewed for reuse. This limits the potential for applicative exploitation of the present system. Different immobilization strategies for M80A are thus needed to improve protein film stability, persistence of the biocatalyic effect, and durability of the amperometric detection.

Conclusions

Replacement of the axial heme iron methionine ligand with a noncoordinating Ala residue in cytochrome *c* dramatically affects the thermodynamics and kinetics of heme Fe(III) to Fe(II) reduction for the electrode-immobilized protein at neutral pH compared to the native species. The electrochemical features, the reduction thermodynamics, and the ET kinetics investigated in different conditions of pH are dominated by the presence of a hydroxide ion in place of the native methionine as the sixth axial ligand of Fe(III), which dissociates upon electron uptake. The change in axial heme iron coordination between OH^- and water is the main determinant of the pH-induced changes in the thermodynamic and kinetic ET parameters observed with both SAMs below pH 6, since the distances of ET between the heme and the electrode are found to be independent of pH. The M80A mutation does not sensibly modify the interaction with the 1:1 mixed 11-MUAc/11-MUAl SAMs compared to the native cytochrome *c*, confirming its limited impact on the overall protein structure. On the other hand, the distance of ET between the heme and the electrode coated with 4-MP is consistent with the involvement of at least one solvent molecules in the hydrogen-bond network at the interface between the protein and the layer. Probably, the most intriguing feature of the immobilized M80A cytc layer is its ability to act as an efficient biocatalyst for O_2 reduction between pH 5 and 11.0, which opens the way to the exploitation of this cytochrome *c* mutant for O_2 biosensing. On these bases, once the problem of protein film stability is solved, the open coordination heme site in M80A may serve as biocatalytic center for the amperometric detection of other chemicals of environmental or clinical interest, such as NO, NO_2^-, CO, etc. As a perspective, additional mutations in the proximal and distal heme site of cytc aimed at transforming cytochrome *c* in a chimeric peroxidase[65,66] will be worth investigating for the assembly of a biocatalytic surface for the bio-based detection of hydrogen peroxide, of use for monitoring the cellular oxidative stress.

Acknowledgment. This work was supported by the University of Modena and Reggio Emilia (Fondo di Ateneo per la Ricerca 2006).

References and Notes

(1) Armstrong, F. A.; Wilson, G. S. *Electrochim. Acta* **2000**, *45*, 2623−2645.
(2) Fedurco, M. *Coord. Chem. Rev.* **2000**, *209*, 263−331.
(3) Xu, J.; Bowden, E. F. *J. Am. Chem. Soc.* **2006**, *128*, 6813−6822.
(4) Tarlov, M. J.; Bowden, E. F. *J. Am. Chem. Soc.* **1991**, *113*, 1847−1849.
(5) El Kasmi, A.; Wallace, J. M.; Bowden, E. F. *J. Am. Chem. Soc.* **1998**, *120*, 225−226.
(6) Murgida, D. H.; Hildebrandt, P. *J. Phys. Chem. B* **2001**, *105*, 1578−1586.
(7) Heering, H. A.; Wiertz, F. G. M.; Dekker, C.; de Vries, J. *J. Am. Chem. Soc.* **2004**, *126*, 11103−11112.
(8) Bortolotti, C. A.; Battistuzzi, G.; Borsari, M.; Facci, P.; Ranieri, A.; Sola, M. *J. Am. Chem. Soc.* **2006**, *128*, 5444−5451.
(9) Nahir, T. M.; Bowden, E. F. *J. Electroanal. Chem.* **1996**, *410*, 9−13.
(10) Clark, R. A.; Bowden, E. F. *Langmuir* **1997**, *13*, 559−565.
(11) Tanimura, R.; Hill, M. G.; Margoliash, E.; Niki, K.; Ohno, H.; Gray, H. B. *Electrochem. Solid-State Lett.* **2002**, *5*, E67−E70.
(12) Niki, K.; Hardy, W. R.; Hill, M. G.; Li, H.; Sprinkle, J. R.; Margoliash, E.; Fujita, K.; Tanimura, R.; Nakamura, N.; Ohno, H.; Richards, J. H.; Gray, H. B. *J. Phys. Chem. B* **2003**, *107*, 9947−9949.
(13) Imabayashi, S.; Mita, T.; Kakiuchi, T. *Langmuir* **2005**, *21*, 1470−1474.
(14) Petrovic, J.; Clark, R. A.; Yue, H. J.; Waldeck, D. H.; Bowden, E. F. *Langmuir* **2005**, *21*, 6308−6316.
(15) Collinson, M.; Bowden, E. F. *Langmuir* **1992**, *8*, 2552−2559.
(16) Matsuda, N.; Santos, J. H.; Takatsu, A.; Kato, K. *Thin Solid Films* **2003**, *438*, 403−406.
(17) Rinaldi, R.; Biasco, A.; Cingolani, G.; Cingolani, R.; Alliata, D.; Andolfi, L.; Facci, P.; De Rienzo, F.; Di Felice, R.; Molinari, E.; Verbeet, M.; Canters, G. *Appl. Phys. Lett.* **2003**, *82*, 472−474.
(18) Habermuller, L.; Mosbach, M.; Schuhmann, W. *Fresenius' J. Anal. Chem.* **2000**, *366*, 560−568.
(19) Stayton, P. S.; Olinger, J. M.; Jiang, M.; Bohn, P. W.; Sligar, S. G. *J. Am. Chem. Soc.* **1992**, *114*, 9298−9299.
(20) Gerunda, M.; Bortolotti, C. A.; Alessandrini, A.; Sola, M.; Battistuzzi, G.; Facci, P. *Langmuir* **2004**, *20*, 8812−8816.
(21) Banci, L.; Bertini, I.; Bren, K. L.; Gray, H. B.; Turano, P. *Chem. Biol.* **1995**, *2*, 377−383.
(22) Banci, L.; Bertini, I.; Bren, K. L.; Gray, H. B.; Sompornpisut, P.; Turano, P. *Biochemistry* **1995**, *34*, 11385−11398.

(23) Lu, Y.; Casimiro, D. R.; Bren, K. L.; Richards, J. H.; Gray, H. B. *Proc. Natl. Acad. Sci. U.S.A.* **1993**, *90*, 11456−11459.
(24) Bren, K. L.; Gray, H. B. *J. Am. Chem. Soc.* **1993**, *115*, 10382−10383.
(25) Bren, K. L.; Gray, H. B. *J. Inorg. Biochem.* **1993**, *51*, 111.
(26) Barker, P. D.; Bertini, I.; Del Conte, R.; Ferguson, S. J.; Hajieva, P.; Tomlinson, E.; Turano, P.; Viezzoli, M. S. *Eur. J. Biochem.* **2001**, *268*, 4468−4476.
(27) Battistuzzi, G.; Borsari, M.; Ranieri, A.; Sola, M. *Arch. Biochem. Biophys.* **2002**, *404*, 227−233.
(28) Laviron, E. *J. Electroanal. Chem.* **1979**, *101*, 19−28.
(29) Yee, E. L.; Cave, R. J.; Guyer, K. L.; Tyma, P. D.; Weaver, M. J. *J. Am. Chem. Soc.* **1979**, *101*, 1131−1137.
(30) Yee, E. L.; Weaver, M. J. *Inorg. Chem.* **1980**, *19*, 1077−1079.
(31) Taniguchi, V. T.; Sailasuta-Scott, N.; Anson, F. C.; Gray, H. B. *Pure Appl. Chem.* **1980**, *52*, 2275−2281.
(32) Battistuzzi, G.; Bortolotti, C. A.; Borsari, M.; Di Rocco, G.; Ranieri, A.; Sola, M. *J. Phys. Chem. B* **2007**, *34*, 10281−10287.
(33) Chen, X.; Ferrigno, R.; Yang, J.; Whitesides, G. M. *Langmuir* **2002**, *18*, 7009−7015.
(34) Song, S.; Clark, R. A.; Bowden, E. F.; Tarlov, M. J. *J. Phys. Chem.* **1993**, *97*, 6564−6572.
(35) Collinson, M.; Bowden, E. F.; Tarlov, M. J. *Langmuir* **1992**, *8*, 1247−1250.
(36) Hildebrand, P.; Murgida, D. H. *Bioelectrochemistry* **2002**, *55*, 139−143.
(37) Armstrong, F. A. *Struct. Bonding* **1990**, *72*, 136−221.
(38) Louie, G. V.; Brayer, G. D. *J. Mol. Biol.* **1990**, *214*, 527−555.
(39) Fleming, B. D.; Tian, Y.; Bell, S. G.; Wong, L. L.; Urlacher, V.; Hill, H. A. O. *Eur. J. Biochem.* **2003**, *270*, 4082−4088.
(40) Wackerbarth, H.; Murgida, D. H.; Oellerich, S.; Döpner, S.; Rivas, L.; Hildebrand, P. *J. Mol. Struct.* **2001**, *51*, 563−564.
(41) Battistuzzi, G.; Borsari, M.; Francia, F.; Sola, M. *Biochemistry* **1997**, *36*, 16247−16258.
(42) Battistuzzi, G.; Borsari, M.; Sola, M. *Eur. J. Inorg. Chem.* **2001**, 2989−3004.
(43) Battistuzzi, G.; Borsari, M.; Cowan, J. A.; Eicken, C.; Loschi, L.; Sola, M. *Biochemistry* **1999**, *38*, 5553−5562.
(44) Battistuzzi, G.; Borsari, M.; Loschi, L.; Sola, M. *J. Biol. Inorg. Chem.* **1999**, *4*, 601−607.
(45) Battistuzzi, G.; Borsari, M.; Sola, M. *Antioxid. Redox Signaling* **2001**, *3*, 279−291.
(46) Battistuzzi, G.; Borsari, M.; Cowan, J. A.; Ranieri, A.; Sola, M. *J. Am. Chem. Soc.* **2002**, *124*, 5315−5324.
(47) Battistuzzi, G.; Borsari, M.; Ranieri, A.; Sola, M. *J. Biol. Inorg. Chem.* **2004**, *9*, 781−787.
(48) Baistrocchi, P.; Banci, L.; Bertini, I.; Turano, P.; Bren, K. L.; Gray, H. B. *Biochemistry* **1996**, *35*, 13788−13796.
(49) Banci, L.; Bertini, I.; Bren, K. L.; Gray, H. B.; Sompornpisut, P.; Turano, P. *Biochemistry* **1997**, *36*, 8992−9001.
(50) Silkstone, G. G.; Cooper, C. E.; Svistunenko, D.; Wilson, M. T. *J. Am. Chem. Soc.* **2005**, *127*, 92−99.
(51) Silkstone, G. G.; Stanway, G.; Brzezinski, P. T.; Wilson, M. T. *Biophys. Chem.* **2002**, *98*, 65−77.
(52) Nahir, T. M.; Clark, R. A.; Bowden, E. F. *Anal. Chem.* **1994**, *66*, 2595−2598.
(53) Marcus, R. A.; Sutin, N. *Biochim. Biophys. Acta* **1985**, *811*, 265−322.
(54) Weaver, M. J. *J. Phys. Chem.* **1979**, *13*, 1748−1757.
(55) Becka, A. M.; Miller, C. J. *J. Phys. Chem.* **1992**, *96*, 2657−2668.
(56) Finklea, H. O.; Hanshew, D. D. *J. Am. Chem. Soc.* **1992**, *114*, 3173−3181.
(57) Murgida, D. H.; Hildebrand, P. *J. Mol. Struct.* **2001**, *97*, 565−566.
(58) Feng, Z. Q.; Imabayashi, S.; Kakiuchi, T.; Niki, K. *J. Electroanal. Chem.* **1995**, *394*, 149−154.
(59) Dick, L. A.; Haes, A. J.; van Duyne, P. *J. Phys. Chem. B* **2000**, *104* 11752−11762.
(60) Leopold, M. C.; Bowden, E. F. *Langmuir* **2002**, *18*, 2239−2245.
(61) Cheng, J.; Miller, C. J. *J. Phys. Chem. B* **1997**, *101*, 1058−1062.
(62) Wenger, O. S.; Leigh, B. S.; Villahermosa, R. M.; Gray, H. B.; Winkler, J. R. *Science* **2005**, *307*, 99−102.
(63) Bendall, D. S. *Protein Electron Transfer*; BIOS Scientific: Oxford, 1996; Chapters 1 and 2.
(64) Moser, C. C.; Dutton, P. L. *Biochim. Biophys. Acta* **1992**, *1101*, 171−176.
(65) Wang, Z.-H.; Lin, Y.-W.; Rosell, F. I.; Ni, F.-Y.; Lu, H.-J.; Yang, P.-Y.; Tan, X.-S.; Li, X.-Y.; Huang, Z.-X.; Mauk, A. G. *ChemBioChem* **2007**, *8*, 607−609.
(66) Lu, Y.; Berry, S. M.; Pfister, T. D. *Chem. Rev.* **2001**, *101*, 3047−3080.
(67) Ozaki, S.-I.; Roach, M. P.; Matsui, T.; Watanabe, Y. *Acc. Chem. Res.* **2001**, *34*, 818−825.